THE JOURNAL OF PHYSICAL CHEMISTRY B

Article

pubs.acs.org/JPCB

Reducing Strain and Fracture of Electrophoretically Deposited CdSe Nanocrystal Films. I. Postdeposition Infusion of Capping Ligands

Theodore J. Kramer,[†] Sanat K. Kumar,[‡] Michael L. Steigerwald,[§] and Irving P. Herman*[,†]

[†]Department of Applied Physics and Applied Mathematics, [‡]Department of Chemical Engineering, and [§]Department of Chemistry, Columbia University, New York, New York 10027, United States

Supporting Information

ABSTRACT: Thick electrophoretically deposited (EPD) films of ligand-capped colloidal nanocrystals that adhere to the substrate typically crack after they are removed from the deposition solvent due to the loss of residual solvent. We report the suppression of fracture in several micrometers thick EPD films of CdSe nanocrystals by treating the wet, as-deposited films with solutions containing the NC core-capping ligand, trioctylphosphine oxide (TOPO). The increase in TOPO ligand density increases photoluminescence of the dried film and leads to a decrease in elastic modulus.

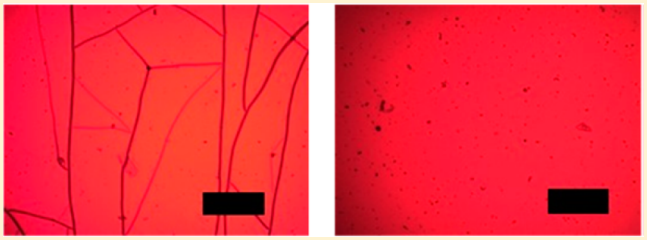

1. INTRODUCTION

The ability to deposit dense conformal colloidal nanocrystal (NC) films using electrophoretic deposition (EPD) could be useful for a variety of applications requiring functionalization of macroscopic surfaces with the unique physical properties (optical, electrical, and magnetic) of nanoscale structures, for one type of particle[1] and for particle mixtures.[2] As such, the goal of the EPD of colloidal, ligand-capped, so-called "colloidal" nanoparticles to form films in which the particles largely maintain their identities[3] differs from that of the EPD of stabilized nanoparticles without ligands to make dense films of the particle material.[4−6] Previous work has shown that EPD films of colloidal cadmium selenide (CdSe) NCs are highly photoluminescing and deposit with high spatial selectivity on patterned conductive substrates.[1] These same studies showed that EPD films composed of 2−4 nm diameter CdSe NCs fracture when films that are thicker than ∼600−800 nm are removed from the deposition solvent.[1,7,8] This occurs as a result of the stresses and strain that develop in the film, which still adheres to the substrate, when the residual solvent present after EPD evaporates. The resulting cracks typically extend through the film thickness and expose the underlying substrate and, for very thick films, partially delaminate. This poses an obstacle to the use of EPD films of NCs or any nanoparticles in applications such as sensors, photovoltaics, and emissive displays, where standard fabrication techniques after film deposition would result in shunt pathways and nonuniform device performance. We show how to suppress fracture in EPD CdSe NC films by bathing them in solutions of trioctylphosphine oxide (TOPO), one of the ligands that caps the CdSe NC core, prior to the drying of the deposition solvent. The increased photoluminescence (PL) efficiency of these films indicates that at least part of the infused TOPO binds to open sites on the CdSe cores.

The equilibrium NC separation in the EPD film decreases as a result of the evaporation of the residual deposition solvent in the already-formed EPD film, a separation that is determined by the balance between attractive inter-NC van der Waals forces and repulsive forces from ligand−ligand steric interference. However, the NC separation is fixed when the film adheres during drying, so in-plane tensile strain increases and, for large enough strains, fracture can occur.[1,7,8] Such fracture due to solvent evaporation also occurs in drop-cast NC films. Eliminating cracking is also important in forming uniform, dense ceramic films by the EPD of stabilized nanoparticles without ligands.[6]

In the several-step washing procedure needed to prepare the NCs to form the EPD films,[9] a fraction of the short-chain phosphonic acid and TOPO capping ligands is removed;[9,10] it is thought that phosphonic acids are the primary coordinating ligands. However, this washing procedure may increase the amount of residual solvent in the as-deposited film, which will increase tensile strain in the dried film and the likelihood of fracture. Previous studies of fracture of EPD NC films have determined the in-plane tensile strain due to drying and observed the drying and fracture in real time.[7,8]

The infusion of TOPO both onto vacant binding sites on the cores and into interstitial regions between the cores while the EPD CdSe NC film is still in solution could lessen the film strain that appears after drying. This, along with concomitant changes in film mechanical properties, may suppress film fracture. We demonstrate that this procedure does indeed suppress fracture.

Special Issue: Electrophoretic Deposition

Received: June 7, 2012
Revised: August 27, 2012
Published: September 6, 2012

2. EXPERIMENTAL METHODS

All materials were obtained from Sigma-Aldrich and used without purification.

The synthesis of CdSe NCs followed a procedure adapted from ref 11. A solution of TOPO was combined with tetradecylphosphonic acid (TDPA) and heated to 350 °C. A solution of trioctylphosphine-selenide (TOP-Se) and dimethylcadmium was rapidly injected. and the solution was held at 280 °C for 20 min. The average NC diameter was 4.0 nm, as determined by UV−vis absorption spectroscopy[12] and confirmed using transmission electron microscopy. (See the Supporting Information for more details about synthesis and other aspects of film preparation.)

CdSe NCs were subjected to four cycles of centrifugal precipitation (washing) and dissolution using methanol and hexane, respectively. The final CdSe NC solution (in hexane) was used to deposit the EPD film on prescored gold-coated (~10 nm chromium/50 nm gold) silicon electrodes by applying 800 V across the electrodes, separated by 2 cm, for 10 min. EPD films formed on both electrodes with approximately the same thickness.[1]

Following deposition, the positive and negative electrodes were quickly moved to baths of hexane. Each electrode was split along predefined score lines, and the resulting pieces were removed and quickly immersed in solutions of 0 (the control or untreated film), 5, 10, 15, 20, and 30 mM of TOPO in hexane for 30 min. (Film properties did not change with even longer immersions.) EPD films were removed from the TOPO solutions and allowed to dry in air.

Film thicknesses were measured with a Dektak mechanical profilometer.[13] The elastic moduli of the films were measured using an Agilent G200 nanoindenter equipped with a standard diamond Berkovich tip that oscillated at 40 Hz and driven to a depth of 1000 nm in the continuous stiffness measurement (CSM) mode, with a tip advancement of 0.2 nm per cycle (8 nm/s). Elastic moduli[14,15] were averaged from 200 to 250 nm into the films and were determined assuming a film Poisson ratio $\nu = 0.18$ but the obtained moduli were insensitive to the choice of ν used for data analysis (Figure S1 in the Supporting Information). The viscous response is described by the out-of-phase component, the loss modulus. This is presented for the films, as is usual, by the phase angles,[14,15] $\tan^{-1}$(loss modulus/elastic modulus), which were determined at 800 nm depth. PL was measured using 514.5 nm excitation from a Melles Griot cw argon-ion laser.

3. RESULTS

Untreated EPD CdSe NC films grown to a thickness of ~2.25 μm (>fracture thickness threshold) exhibited a dense network of channel cracks across the film thickness.[8] Figure 1 shows that the TOPO treatment suppresses fracture in the positive electrode film, and Figure S2 in the Supporting Information shows this for the negative electrode film. When treated with solutions of 5 and 10 mM TOPO, EPD CdSe NC films form fine cracks. Films treated with TOPO concentrations ≥15 mM do not crack.

Figure 2 shows an increase in film thickness with TOPO concentration of up to 38% (for 30 mM TOPO). Most of the change in film thickness occurs in treatments with ≤15 mM TOPO.

Figure 3 shows a typical nanoindentation trace for the negative electrode film; those of the positive electrode film look similar (Figure S3 in the Supporting Information). The elastic modulus E of untreated EPD CdSe NC films ranges from 7.5 to 9.5 GPa; this is consistent with results from previous studies.[13] These dried films show a dramatic decrease in E upon treatment of films with TOPO (Figure 4a). Most of this softening occurs for treatment with <15 mM. With this decrease in E, there is a concomitant increase in phase angle and therefore viscoelasticity (Figure 4b).

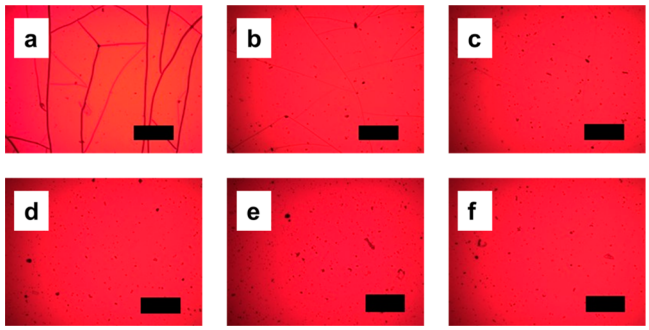

Figure 1. Optical micrographs of EPD CdSe NC films on the positive electrode treated with (a) 0, (b) 5, (c) 10, (d) 15, (e) 20, and (f) 30 mM TOPO. The scale bar is 500 μm wide.

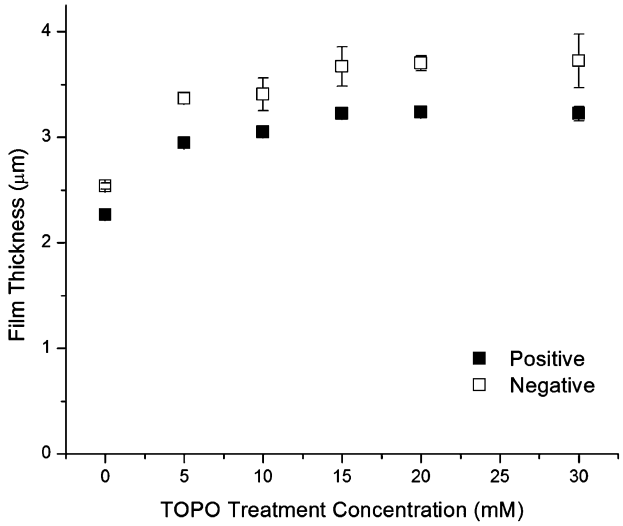

Figure 2. Film thickness after TOPO treatment and drying of the positive and negative electrode films.

TOPO solution treatment of EPD CdSe NC films greatly increases the NC PL efficiency for films on both electrodes (and for this sample, more so on the negative electrode film, Figure 5). PL signals slowly increase with further increase in TOPO concentration, and the increase saturates for TOPO concentrations of ≥15 mM. (However, there is a loss of PL intensity for the negative electrode film with 30 mM TOPO treatment that might be related to the pure TOPO deposits that accumulate on the film surface only for that condition.)

The Supporting Information includes results from other runs in which the EPD films were made using particles synthesized using either similar or slightly different procedures. They show the same trends: the TOPO solution treatment reduces or, at high enough concentrations, suppresses film cracking, decreases the film elastic modulus and increase viscoelasticity, and increases film PL (which is approximately the same for the films on both electrodes, Figure S11 in the Supporting Information). Increases in film thickness with TOPO treatment

dx.doi.org/10.1021/jp305607t | J. Phys. Chem. B 2013, 117, 1537−1543

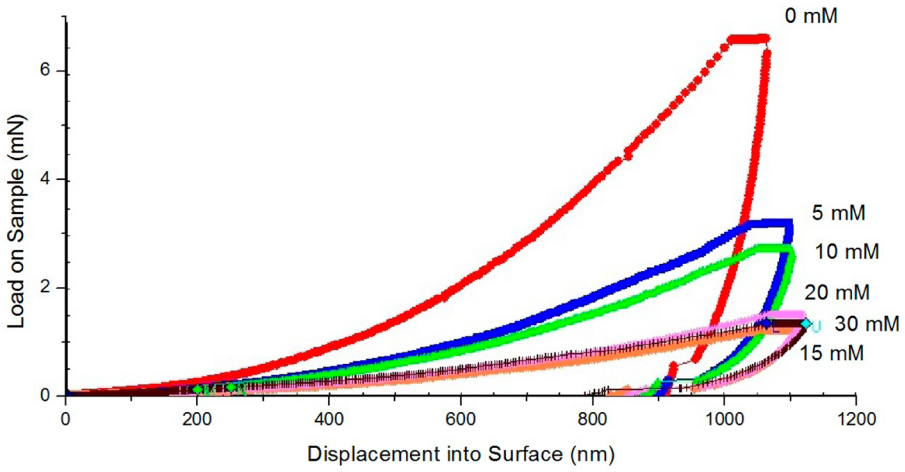

Figure 3. Nanoindenter force–displacement plots (8 nm/s) for the negative electrode film after treatment by the TOPO solutions and drying.

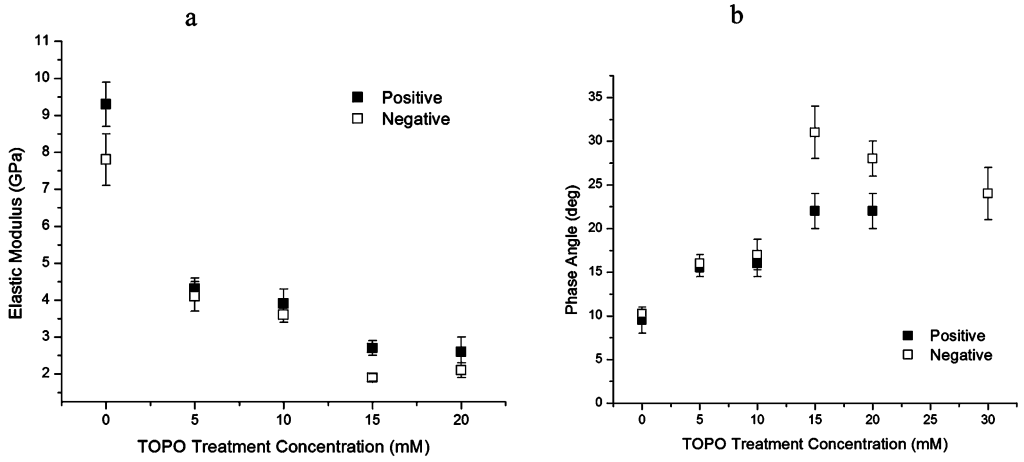

Figure 4. (a) Elastic modulus and (b) phase-angle measurements of TOPO-treated EPD films.

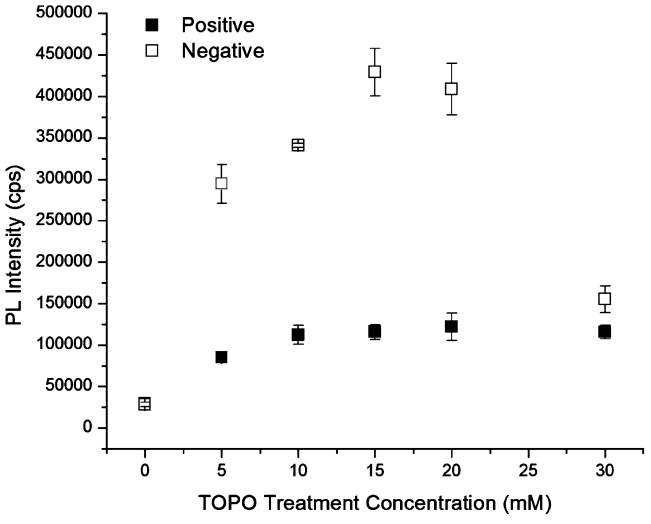

Figure 5. Normalized PL efficiency of TOPO-treated EPD CdSe NC films.

concentration are generally seen (Figures S4 and S8 in the Supporting Information); however, there is more scatter in the data of those runs, perhaps because of the differences in film preparation or the smaller sizes of the NC cores used. The films grown on the positive and negative electrodes always have roughly the same thickness and have similar properties that qualitatively change the same way with TOPO treatment. Of note, in each case they both do not fracture for ≥15 mM TOPO treatment.

Figure S12 in the Supporting Information shows the nanoindentation trace of a dried and cracked EPD film remains largely unchanged if it is then soaked in 30 mM TOPO for 2 h and dried again. Also, after this treatment the cracks are still present and the PL is essentially unchanged (Figure S13 in the Supporting Information). Therefore, TOPO infusion can occur in the EPD film after it is formed and still wet but not after it has dried.

Use of other ligands was briefly surveyed. Instead of treating the still wet phosphonic acid/TOPO-capped CdSe NC EPD film in TOPO solution, it was soaked in 30 mM hexadecylamine in hexane. The film quickly lifted off of the substrate and broke into very small pieces and precipitated instead of redissolving fully into solution. In a separate experiment, the CdSe NCs were refluxed in hexadecylamine to change from phosphonic acid and TOPO ligands to hexadecylamine ligands, but these NCs did not form EPD films.

4. DISCUSSION

4.1. Overview of Film Properties. All changes in film conditions and properties (lessened propensity to fracture, increased PL, decreased elastic modulus, increased viscoelas-

dx.doi.org/10.1021/jp305607t | J. Phys. Chem. B 2013, 117, 1537–1543

ticity, and generally increased thickness) indicate significant intake of TOPO into the EPD film when it is treated while it is still wet. The changes are saturated when TOPO treatment concentrations are increased to concentrations as high as ∼10−15 mM. There does not seem to be significant TOPO intake into the film when it is treated after it has dried, likely because NC rearrangement after drying narrows the inter-NC regions.

Most of these changes could be due to increased density of TOPO bound to the cores and unbound in the voids. Only the increase in PL, due to surface passivation, is definitive proof that at least some of the infused TOPO increases ligand density bound to the cores. Moreover, because PL no longer increases for treatments >15 mM TOPO, all available sites for capping ligands appear to be filled by treatment with 15 mM TOPO. It would not be surprising if most of the infused TOPOs were bound to the cores.

There are clearly voids in the structure occupied by solvent while wet and by air when dry. If not, there would not be large strains and fracture in the dried untreated film and there would not be the apparently facile diffusion of TOPO into the wet film. In Section 4.6 it is argued that the decrease in E due to TOPO treatment suggests (very local) rearrangement of the NCs in the film, particularly away from the substrate.

It is assumed that composition and properties do not change with depth into the film. It is possible that there is a gradient in TOPO diffusion and deposition, and in film properties with depth into the film, and that TOPO infusion into the upper part of the film could lessen diffusion to the film near the substrate. Although this might play a role in a local rearrangement of NCs just mentioned, there is no reason to believe that this dominates observations here, and it is not further considered.

4.2. Ligand Shells. We model the TOPO ligands on CdSe NCs in solution, as in refs 16 and 17, as truncated cones with 0.252 nm radius (0.2 nm^2 area) apex bases on the core surface, heights (= the ligand shell thickness) of l_{wet} = 0.99 nm (∼ 1 nm), and base radii on the shell of 0.55 nm (the small number of phosphonic acid ligands remaining after NC washing is ignored). The maximum TOPO coverage density increases for smaller cores[16,17] due to lessened steric hindrance. For a 4 nm diameter core (core radius r = 2 nm), up to ∼30% of the core surface can be covered by ligands (∼75 ligands). Approximating the TOPO molecule volume by the cone volume, 0.53 nm^3, the maximum fraction of the shell that can be occupied by ligands can be estimated to be the ratio of the total volume of the cones divided by the ligand shell volume, which is ∼0.5 for 4 nm NCs. When all solvent evaporates during drying except that in the ligand shell, the separation between the surfaces of near-neighbor cores could range between 1 (for total interdigitation of the ligand shells) and 2 nm (for no interdigitation).

After drying, the ligands of an individual NC will contract to the core; if this retraction occurred to maximize ligand density on the core and all ligand sites were occupied, then the shell thickness would be 0.6 nm. So, when NC solutions are dropcast and allowed to dry, the minimum separation of the fully capped cores would then be twice this thickness, ∼1.2 nm, for this fully dense TOPO matrix, which would correspond to either maximum ligand interdigitation or core/shells acting as hard spheres.

For the multiply washed NCs, which have fewer than the maximum number of ligands on the core, the ligand shell thickness while wet is still expected to be ∼1.0 nm, the extended length of a TOPO molecule. If the PL intensity were proportional to ligand coverage, as is suggested in ref 18, then the 4−15 fold increase in PL intensity seen in Figures 5 and Figures S7 and S11 of the Supporting Information would suggest that there is ∼10−25% of the maximum (30%) ligand coverage without TOPO treatment. With maximum ligand retraction, the shell thickness after drying would be l_{dry} = 0.47/0.33/0.18/0.08 nm, respectively, for 75/50/25/10% of the maximum (30%) ligand coverage.

These are low-end estimates of the shell thicknesses of the dried NC because contraction is limited by steric effects and because the estimated molecular volume in this model (∼0.52 nm^3) is smaller than the estimated molecular volume of TOPO (∼0.71 to 0.80 nm^3, using a bulk density of ∼0.8 to 0.9 g/cm^3 is typical of organic molecules). Also, for ligand areal density n, the thickness of long polymer brushes (which is equated to ligand shell thickness here) $l_{dry} = A(Bn)^{\eta}$, where η has been found to be 1/3 by ref 19 and 1/2 by ref 20. In this maximum ligand retraction model, the effective η varies from ∼1/3, for larger ratios of the ligand shell thickness to core radius and higher surface coverages, to ∼1, for smaller ratios of the ligand shell thickness to core radius and smaller surface coverages. Also note the uncertainty of the assumption that l_{wet} = 0.99 nm.

4.3. EPD Film Formation, Drying, and Strain Evolution. During EPD, the nearest separation between core surfaces of nearest neighbor NCs could range between $a_{eq,wet}$ = 1.0 and 2.0 nm ($a_{eq,wet} = \alpha_{wet} l_{wet}$, where α_{wet} ranges from 1 to 2). (Total interdigitation, with α_{wet} = 1, would be possible for ≤80% of the maximum (30%) ligand coverage, for which the thickness of retracted ligand shell is ≤0.5 nm; this condition is expected for the multiply washed NCs used in EPD.) After drying, the core separation would still be $a_{eq,wet} = \alpha_{wet} l_{wet}$ for the adhering film, at least near the substrate.

For NCs with cores of radius r with the cores separated by distance a, and a_{eq} in equilibrium, the in-plane strain is

$$\varepsilon = \frac{a - a_{eq}}{2r + a_{eq}} \tag{1}$$

For the adhering film, $a = a_{eq,wet} = \alpha_{wet} l_{wet}$. As a result of drying, the ligand shell thickness for an isolated NC, l_{dry} (with no TOPO treatment), decreases as the ligands bind to each other and the core. Even though α can increase due to drying, to α_{dry}, the new equilibrium spacing $a_{eq,dry} = \alpha_{dry} l_{dry}$ decreases, and there is in-plane strain in the adhering film of

$$\varepsilon_{dry} = \frac{a_{eq,wet} - a_{eq,dry}}{2r + a_{eq,dry}} = \frac{\alpha_{wet} l_{wet} - \alpha_{dry} l_{dry}}{2r + \alpha_{dry} l_{dry}} \tag{2}$$

This can lead to fracture.

As a result of the TOPO treatment, the equilibrium spacing in the dried film increases to $a_{eq,dry,TOPO} = \alpha_{dry,TOPO} l_{dry,TOPO}$ because with more capping ligands the ligand shell becomes thicker, so $l_{dry,TOPO} > l_{dry}$ and also $\alpha_{dry,TOPO} \geq \alpha_{dry}$. The TOPO treatment decreases the in-plane tensile strain of the dried film to

$$\varepsilon_{dry,TOPO} = \frac{a_{eq,wet} - a_{eq,dry,TOPO}}{2r + a_{eq,dry,TOPO}} = \frac{\alpha_{wet} l_{wet} - \alpha_{dry,TOPO} l_{dry,TOPO}}{2r + \alpha_{dry,TOPO} l_{dry,TOPO}} \tag{3}$$

dx.doi.org/10.1021/jp305607t | J. Phys. Chem. B 2013, 117, 1537−1543

assuming TOPO caps the cores and there is negligible unbound TOPO in the voids. TOPO infusion will not increase $a_{eq,dry,TOPO}$ beyond $a_{eq,wet}$ because whereas infusion is expected to decrease tensile strain, it is not expected to lead to compressive strain.

4.4. Strain and Thickness of EPD Films. We assume the extreme, yet physically reasonable conditions of total interdigitation (α_{wet} = 1) of NCs with thinner ligand shells before drying and maximum ligand retraction afterward and no intermixing of ligand shells ($\alpha_{dry,TOPO} = \alpha_{dry}$ = 2) after drying.

For the untreated films, in the limit of very small ligand shell thickness (approaching zero) after drying, eq 2 shows that ε_{dry} = 0.2 for $a = a_{eq,wet} = l_{wet}$ = 1.0 nm and ε_{dry} = 0.33 for $a = a_{eq,wet} = 2l_{wet}$ = 2.0 nm for r = 2 nm. The Langrangian strains in the EPD films of ref 8 before fracture were estimated to be: $\varepsilon_{dry} \approx 0.98 \pm 0.15$ for r = 1.15 nm CdSe NCs, $\varepsilon_{dry} \approx 0.39 \pm 0.2$ for r = 1.6 nm NCs, and $\varepsilon_{dry} \approx 0.1$ (lower limit estimate) for r = 2.5 nm NCs. In the limit of zero ligand coverage, eq 2 shows that in that study ε_{dry} could range between 0.30 and 0.47, 0.24 and 0.38, and 0.17 and 0.29, within the limits for a for the three NC sizes, respectively, which is consistent with the well-characterized observations for the larger two NCs.

In classical materials, the out-of-plane strain is $\varepsilon_{out} = -[2\nu/(1-\nu)]\varepsilon$ for the condition of plane stress, where ν is the Poisson ratio. If NC solids were classical in this sense, then TOPO infusion would fractionally increase the thickness of the dried EPD film by

$$\varepsilon_{out,dry,TOPO} - \varepsilon_{out,dry} = -\frac{2\nu_{dry,TOPO}}{1-\nu_{dry,TOPO}}\varepsilon_{dry,TOPO} + \frac{2\nu_{dry}}{1-\nu_{dry}}\varepsilon_{dry} \quad (4)$$

If the film that had been treated with 30 mM TOPO were unstrained when dry ($\varepsilon_{dry,TOPO}$ = 0), the ~38% expansion in film thickness due to the treatment in Figure 2 could be explained by a tensile strain ε_{dry} = ~0.45 for ν = 0.3 or ~0.89 for ν = 0.18 in the untreated, dried film (before fracture). This would be consistent with the results of ref 8.

However, in these nontraditional materials,[21] ν might be very small (and approach zero) or be poorly defined because of the ligand structure in NC films. Whereas the in-plane separations of NCs may not change after solvent evaporation and ligand shell contraction because of film adhesion, the separation of layers of NCs parallel to the substrate may decrease until the ligand shells make contact. With this hard sphere packing of NCs (cores + ligand shells) in the z direction, increasing the ligand shell thickness, as with TOPO treatment, would increase film thickness proportionately by

$$\frac{(2r + a_{eq,dry,TOPO}) - (2r + a_{eq,dry})}{2r + a_{eq,dry}} = \frac{a_{eq,dry,TOPO} - a_{eq,dry}}{2r + a_{eq,dry}} \quad (5)$$

with no other change in structure. In the limit of no pretreatment ligand shell ($a_{eq,dry}$ = 0), this could lead to a fractional thickness increase of 25–50% for $a_{eq,dry,TOPO}$ = 1 to 2 nm, which is also consistent with the observations in Figures 2 and Figures S4 and S8 of the Supporting Information, and a large decrease in (or total loss of) in-plane strain.

4.5. Consideration of Fracture. According to classical fracture theory, cracking occurs in the film whenever the Griffith's criterion[22] is met during any stage of drying. This criterion for channel crack formation is that the film thickness h exceeds the critical film thickness

$$h_c = \frac{\Gamma E}{(1-\nu^2)Z\sigma^2} = \frac{\Gamma(1-\nu)}{(1+\nu)ZE\varepsilon^2} \quad (6)$$

where σ and ε are the in-plane film stress and strain (in the regime in which $\sigma = \varepsilon E/(1-\nu)$ is valid); E, ν, and Γ are the film elastic modulus, Poisson ratio, and toughness; and Z is a parameter = 1.98 for channel cracks.[23] Each of these parameters, except Z, changes during drying.

TOPO treatment of the EPD NC films may prevent fracture, by increasing h_c, because of one or more of the following mechanisms:

(1) Decreased strain due to added capping ligands: The added bound ligands decrease in-plane film strain ε in the dried film and likely in-plane stress σ also. This appears to be important in suppressing fracture. Whereas it is difficult to assess the influence of TOPO treatment on ligand shell thickness and potential void filling (Mechanism 2), the increased PL with TOPO treatment proves that some (if not most or all) of the added TOPO binds to the NC cores.

(2) Decreased strain due to added ligands in interstitial regions: Interstitial regions of the as-deposited film (occupied only by deposition solvent in the wet film without TOPO treatment) could be filled with unbound TOPO (void filling), reducing film contraction ε. This may be important (see above).

(3) Decreased film elastic modulus: The film E is seen to decrease, so σ would decrease even if ε did not (within and near the linear stress–strain regime). This may be important but only if it is not accompanied by a decrease in fracture strength.

(4) Increased film toughness: The infusion and coordination of TOPO likely increases ligand interdigitation. This would increase van der Waals forces and likely increase film toughness (Γ), which would help suppress fracture.

(5) Film overcoating: If the EPD films were overcoated or encapsulated by a film of TOPO, then this could reduce the density of nucleation crack sites in the EPD film and suppress fracture; however, there is no evidence of this. (However, after treatment with the highest TOPO concentration solutions, TOPO crystals do appear on the surface.)

Other mechanisms might be significant as well. Film viscoelasticity increases with TOPO treatment, but it is not clear if this is important in suppressing fracture. TOPO passivates surface-defect sites, which appears to increase the local fracture toughness above the critical fracture threshold. In untreated films, cracks usually originate from small points that appear as black or dark red spots in the film, which may be dense aggregates of poorly passivated NCs. The density of these sites decreases with TOPO treatment, indicating that such passivation does occur; however, they still exist, and fracture still occurs at the lowest TOPO concentrations.

4.6. Evaluating and Modeling the Elastic Modulus. TOPO treatment decreases the elastic modulus from ~9 to ~2.5 GPa (Figure 4). In other runs reported in the Supporting Information, it decreases E from ~5 to ~1.3 GPa (Figure S5) and ~8 to ~1.3 GPa (Figure S9 in the Supporting Information). The variability in the moduli of the untreated

dx.doi.org/10.1021/jp305607t | J. Phys. Chem. B 2013, 117, 1537–1543

and treated films arises from variations under preparation conditions (core radius, ligand shell thickness, and so on), as is seen below.

We will use mean-field micromechanics models of multiphase materials to analyze the elastic modulus E for dried EPD films after TOPO treatment, composed of a filler (the NC core filler, CdSe) in a matrix of a medium (TOPO ligands) and voids. These models, described in the Supporting Information, predict a film E smaller than the average of the elastic moduli of the individual components when weighted by volume fraction. The packing fractions for random close-packed and random loose-packed structures of hard spheres,[24,25] f, are 0.64 and 0.58; random loose-packing is assumed in the models. The models also use the results of a recent study that showed how the elastic modulus of CdSe NC cores decreases with radius[26] ($E_{CdSe} \approx 21.5$ GPa for the 2 nm radius cores here).

The two-phase micromechanics models predict elastic moduli that are the same as that of the voids (0 GPa) for the dried untreated EPD films, when modeled as a loose-packed collection of cores (with vanishingly thin ligand shells) in an air matrix. (This is also true if cores with very thin ligand shells are used with three-phase models.) However, there is of course significant direct contact between cores, more in the vertical direction than in the lateral direction across the substrates due to adhesion.

We use a different approach to account for voids. Christensen[27] showed that spherical voids of volume fraction c_{void} decrease the elastic modulus of a medium E_m as

$$E_{film} = E_m(1 - 2\alpha c_{void}) \quad (7)$$

for small c_{void}, where $\alpha = 3(1 - \nu_m)(9 + 5\nu_m)/4(7 - 5\nu_m)$ and ν_m is the medium Poisson ratio. For $0 \leq \nu_m \leq 0.5$, α is insensitive to ν_m and is ~1. For concentrated voids, $c_{void} \rightarrow 1$

$$E_{film} = E_m[2/(5 + 3\nu_m)](1 - c_{void}) \quad (8)$$

(See the Supporting Information for a previous treatment of voids.[28]) Modeling the untreated, dried EPD film as a medium with elastic modulus 21.5 GPa (that of the CdSe core) with c_{void} = 0.42 for loose-packed CdSe cores gives a film elastic modulus between 3.4 and 4.5 GPa, as bounded by eqs 7 and 8, which is lower than that measured. For packing fractions approaching close packing f = 0.74, eq 7 (is reasonably valid and) gives an elastic constant ~10.3 GPa. This is more consistent with observations, but tight packing is not expected given that the NCs are not ordered and is not consistent with the large strains. Still, such films may be understood by an intermediate degree of core packing.

If the TOPO treatment merely replaced these air voids with TOPO in the still wet EPD films, then E would be larger in the dried treated films than in the dried untreated films because of this ($E_{TOPO} > E_{void}$) and because the fractional volume outside the voids would be expected to decrease. Because a decrease is seen, either the TOPO treatment leads to some rearrangement of NCs and the volume fraction of NC cores decreases or, less likely, the additional TOPO softens the existing TOPO matrix (lowers E_{TOPO}).

After TOPO treatment and the possible local rearrangement of NCs, there are CdSe cores and TOPO ligands and perhaps air voids. In the limit of dominating ligand steric repulsion, the NCs (core of radius r + ligand shell of thickness l) can be treated as hard spheres; for a free film, the fractional volumes of the cores, ligands, and voids would be: $c_{CdSe} = f[r/(r + l)]^3$, $c_{TOPO} = f\{1 - [r/(r + l)]^3\}$, and $c_{void} = (1 - f)$, where f is the packing fraction of NCs.

If the van der Waals attraction forces dominate, then the ligands will protrude into the voids and the core separation will be less than $2l$. If $l > (1/f^{1/3} - 1)r$, then the ligands can fill all of the regions between the cores, with none of them in contact. This corresponds to $l \geq 0.40$ nm for 2 nm radius cores and f = 0.58, or ≥62% of the maximum ligand coverage of the core. In this regime: $c_{CdSe} = [r/(r + l)]^3$ and $c_{TOPO} = 1 - [r/(r + l)]^3$. For l = 0.6, 0.5, and 0.4 nm, c_{CdSe} = 0.45, 0.51, and 0.58 and c_{TOPO} = 0.55, 0.49, and 0.42, with $c_{void} = 0$. If $l < (1/f^{1/3} - 1)r$, then the ligands cannot fill all of the voids, even if the cores touch. Then, for minimum void fractions: $c_{CdSe} = f$, $c_{TOPO} = f\{[(r + l)/r]^3 - 1\}$, and $c_{void} = 1 - f[(r + l)/r]^3$. For l = 0.3, 0.2, and 0.1 nm, c_{CdSe} = 0.58 (always), c_{TOPO} = 0.30, 0.19, and 0.09, and c_{void} = 0.12, 0.23, and 0.33, assuming minimum void volume.

The two-phase (CdSe core "filler" and TOPO medium) Halpsin–Tsai model[29] micromechanics model is used with E_{CdSe} = 21.5 GPa for r = 2 nm. For l ranging from 0.6 (maximum ligand coverage) to 0.4 nm, E_{film} increases from 2.0 to 2.7 GPa with E_{TOPO} = 0.8 GPa, and all Poisson ratios = 0.18; this range is consistent with the results of Figure 4a. These results are not very sensitive to CdSe core elastic modulus or the core and Poisson ratios. They are reproduced using E_{TOPO} = 1.02 GPa for this same two-phase CdSe core/TOPO medium with 10% voids treated by the eq 7 (which we will call the Halpin–Tsai–Christensen three-phase model).

For l ranging from 0.3 to 0.1 nm, this Halpin–Tsai–Christensen model with minimum voids gives a film E of ~2.4 to 2.5 GPa for E_{TOPO} = 0.8 GPa, and all Poisson ratios = 0.18; again this range is consistent with the results of Figure 4a.

This agrees with the measured E for a range of ligand shell thicknesses (0.1 to 0.6 nm), with minimum void fraction, all with E_{TOPO} = 0.8 GPa, but this analysis does not determine the actual shell thickness. Results are also consistent with measurements when larger void fractions are assumed if larger values of E_{TOPO} are used. It is noted that the predictions of other micromechanics models (Cohen–Ishai,[28] Mori–Tanaka,[30] and Christensen–Lo[30]) can vary by ~20%; such model variations do not affect the main conclusions of this study

The somewhat smaller elastic moduli of the untreated EPD films in the Supporting Information are partially explained by the smaller NC core radii (and their smaller elastic moduli,[26] $E_{CdSe} \approx 17$ and 14 GPa for the 1.75 and 1.6 nm radii). The somewhat smaller measured values of the elastic modulus after these films are treated with TOPO (~1.3 GPa) are modeled using their different core sizes and a slightly smaller value of E_{TOPO}, ~0.6 GPa.

Previous nanoindentation analysis of EPD films[7] of CdSe NCs found that the elastic modulus was E = ~8–10 GPa, which is consistent with what is measured here. (E was found to be much smaller, ~2 to 2.5 GPa, after cross-linking the NCs in the EPD film, followed by treatment to remove the TOPO ligands, presumably because of much replacement of TOPO by voids and possibly also larger voids due to larger inter-NC core spacing.) In a related study,[7] the elastic modulus of TOPO in EPD CdSe NC films was estimated to be 2.45 to 4.41 GPa by using Raman spectroscopy and fracture patterns. As seen in the Supporting Information of this article, this is now estimated to be 0.9 to 1.5 GPa using recent data for the elastic modulus of the CdSe NCs.[26]

dx.doi.org/10.1021/jp305607t | J. Phys. Chem. B 2013, 117, 1537–1543

For drop-cast assemblies of NCs, the elastic modulus was found to be ∼6 GPa for 2D array membranes of Au NCs (capped by dodecanethiol),[31] ∼0.2−6 GPa for a range of NC supercrystals,[32] and ∼0.84 and ∼2.16 GPa for CdSe NC films and supercrystals. The effective elastic modulus of the matrix (outside the cores) was estimated in ref 32 to be ∼0.1 to 0.7 GPa for a range of ligand matrices, with ∼0.22 GPa for TOPO in CdSe NC films and ∼0.71 GPa for TOPO in CdSe NC supercrystals.

5. CONCLUSIONS

When large strains and fracture arise after drying of EPD films formed from NCs with incomplete ligand shells on the core, the mechanical state of the film can be substantially improved by recapping the core with ligands before film drying. Specifically, it was seen here that treating EPD CdSe NC films with TOPO solutions reduces or suppresses cracking and concomitantly increases film thickness a bit, reduces the elastic modulus of the film, and greatly increases film PL. Whereas this treatment reduces film strain greatly, there still may be some small residual strain. Film electrical conductivity might also be controllable by the choice of the coordinating ligand that is infused; increasing charge conductivity would be important for several applications of EPD NC films, such as for solar cells[33] and field-effect transistors. The companion paper[34] shows that fracture can also be suppressed by infusing molecules that are not expected to cap the NC cores into the EPD NC film before it dries, specifically monomers that are later polymerized.

■ ASSOCIATED CONTENT

Ⓢ Supporting Information

Further data concerning the sample preparation and properties and modeling. This material is available free of charge via the Internet at http://pubs.acs.org.

■ AUTHOR INFORMATION

Corresponding Author

*E-mail: iph1@columbia.edu.

Notes

The authors declare no competing financial interest.

■ ACKNOWLEDGMENTS

This work was supported by the MRSEC program of the National Science Foundation (DMR-0213574), the NSEC program of the NSF (CHE-0641523), the EFRC program of DoE (DE-SC0001085), and the New York State Office of Science, Technology, and Academic Research (NYSTAR). We thank Derek Huang for help in the experiments.

■ REFERENCES

(1) Islam, M. A.; Herman, I. P. *Appl. Phys. Lett.* **2002**, *80*, 3823−3825.
(2) Islam, M. A.; Xia, Y.; Steigerwald, M. L.; Yin, M.; Liu, Z.; O'Brien, S.; Levicky, R.; Herman, I. P. *Nano Lett.* **2003**, *3*, 1603−1606.
(3) *Electrophoretic Deposition of Nanomaterials*; Dickerson, J. H., Boccaccini, A. R., Eds.; Springer: New York, 2011.
(4) Sarkar, P.; Nicholson, P. S. *J. Am. Ceram. Soc.* **1996**, *79*, 1987−2002.
(5) Van der Biest, O. O.; Vandeperre, L. J. *Annu. Rev. Mater. Sci.* **1999**, *29*, 327−352.
(6) Besra, L.; Liu, M. *Prog. Mater. Sci.* **2007**, *52*, 1−61.
(7) Banerjee, S.; Jia, S.; Kim, D. I.; Robinson, R. D.; Kysar, J.; Bevk, J.; Herman, I. P. *Nano Lett.* **2006**, *6*, 175−180.
(8) Jia, S.; Banerjee, S.; Lee, D.; Bevk, J.; Kysar, J. W.; Herman, I. P. *J. Appl. Phys.* **2009**, *105*, 103513.
(9) Islam, M. A.; Xia, Y.; D. A. Telesca, J.; Steigerwald, M. L.; Herman, I. P. *Chem. Mater.* **2004**, *16*, 49−54.
(10) Jia, S.; Banerjee, S.; Herman, I. P. *J. Phys. Chem. C* **2008**, *112*, 162−171.
(11) Murray, C. B.; Norris, D. J.; Bawendi, M. G. *J. Am. Chem. Soc.* **1993**, *115*, 8706−8715.
(12) Yu, W. W.; Qu, L. H.; Guo, W.; Peng, X. *Chem. Mater.* **2003**, *15*, 2854−2860.
(13) Lee, D.; Jia, S.; Banerjee, S.; Bevk, J.; Herman, I. P.; Kysar, J. *Phys. Rev. Lett.* **2007**, *98*, 0126103.
(14) Herbert, E. G.; Oliver, W. C.; Pharr, G. M. *J. Phys. D: Appl. Phys.* **2008**, *41*, 074021.
(15) Odegard, G. M.; Gates, T. S.; Herring, H. M. *Exp. Mech.* **2005**, *45*, 130−136.
(16) Katari, J. E. B.; Colvin, V. L.; Alivisatos, A. P. *J. Phys. Chem.* **1994**, *98*, 4109−4117.
(17) Bullen, C.; Mulvaney, P. *Langmuir* **2006**, *22*, 3007−3013.
(18) Ji, X.; Copenhaver, D.; Sichmeller, C.; Peng, X. *J. Am. Chem. Soc.* **2008**, *130*, 5726−5735.
(19) Alexander, S. *J. Phys. (Paris)* **1977**, *38*, 983−987.
(20) Manciu, M.; Ruckenstein, E. *Langmuir* **2004**, *20*, 6490−6500.
(21) Greaves, G. N.; Greer, A. L.; Lakes, R. S.; Rouxel, T. *Nat. Mater.* **2011**, *10*, 823−837.
(22) Freund, L. B.; Suresh, S. *Thin Film Materials: Stress, Defect Formation, and Surface Evolution*; Cambridge University Press: Cambridge, U.K., 2003.
(23) Hutchinson, J. W.; Suo, Z. *Adv. Appl. Mech.* **1992**, *29*, 63−191.
(24) Scott, G. D. *Nature* **1960**, *188*, 908−909.
(25) Onoda, G. Y.; Liniger, E. G. *Phys. Rev. Lett.* **1990**, *64*, 2727−2730.
(26) Huxter, V. M.; Lee, A.; Lo, S. S.; Scholes, G. D. *Nano Lett.* **2009**, *9*, 405−409.
(27) Christensen, R. M. *Proc. R. Soc. London, Ser. A* **1993**, *440*, 461−473.
(28) Cohen, L. J.; Ishai, O. *J. Composite Mater.* **1967**, *1*, 390−403.
(29) Halpin, J. C.; Kardos, J. L. *Polym. Eng. Sci.* **1976**, *16*, 344−352.
(30) Christensen, R. M. *J. Mech. Phys. Solids* **1990**, *38*, 379−404.
(31) Mueggenburg, K. E.; Lin, X. M.; Goldsmith, R. H.; Jaeger, H. M. *Nat. Mater.* **2007**, *6*, 656−660.
(32) Podsiadlo, P.; Krylova, G.; Lee, B.; Critchley, K.; Gosztola, D. J.; Talapin, D. V.; Ashby, P. D.; Shevchenko, E. V. *J. Am. Chem. Soc.* **2010**, *132*, 8953−8960.
(33) Salant, A.; Shalom, M.; Hod, I.; Faust, A.; Zaban, A.; Banin, U. *ACS Nano* **2010**, *4*, 5962−5968.
(34) Kramer, T. J.; Kumar, S. K.; Steigerwald, M. L.; Herman, I. P. *J. Phys. Chem. B* **2012**, 10.1021/jp305608f.